The effect of energy director on ultrasonic consolidation of multilayered composites (laminates) made from unidirectional PEEK/CF prepregs

V.O. Alexenko, S.V. Panin
Laboratory of Mechanics of Polymer Composite Materials, Institute of Strength Physics and Materials Science of Siberian Branch of Russian Academy of Sciences, Tomsk, Russia
vl.aleksenko@mail.ru, http://orcid.org/0000-0003-4375-9132
svp@ispms.ru, http://orcid.org/0000-0001-7623-7360

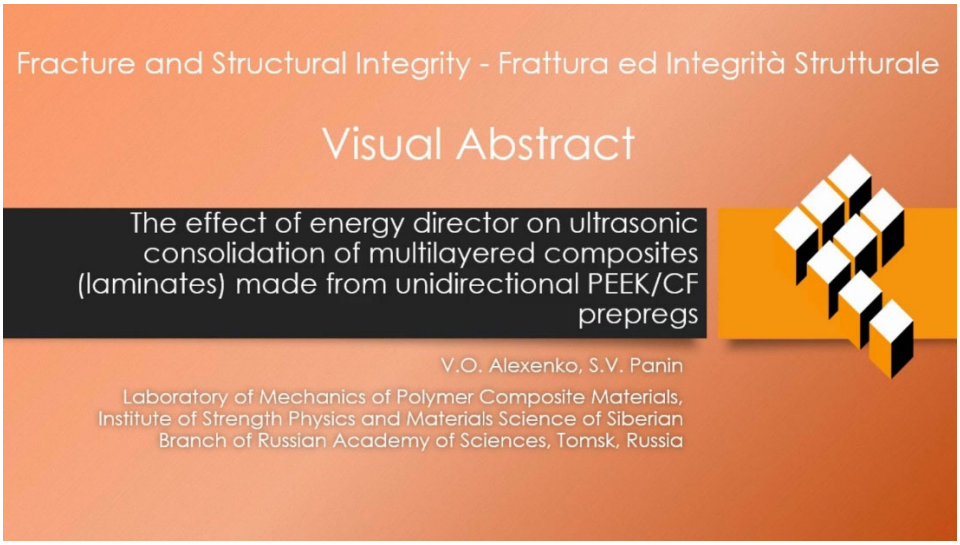

Citation: Alexenko, V.O., Panin, S.V., The effect of energy director on ultrasonic consolidation of multilayered composites (laminates) made from unidirectional PEEK/CF prepregs, Fracture and Structural Integrity, 75 (2026) 315-325.

Received: 09.10.2025
Accepted: 06.11.2025
Published: 12.11.2025
Issue: 01.2026

Copyright: © 2026 This is an open access article under the terms of the CC-BY 4.0, which permits unrestricted use, distribution, and reproduction in any medium, provided the original author and source are credited.

KEYWORDS. Laminated composites, PEEK/CF prepregs, ultrasonic consolidation, interlaminar shear strength, interface, discontinuity.

INTRODUCTION

Fiber-reinforced polymer composites are widely used in aircraft, mechanical and civil engineering, as well as other high-tech industries [1-3]. Their superior strength properties are achieved through loading polymer matrixes with continuous fibers upon the fabrication of layered structures (laminates) [4], which must withstand great impact loads and possess appropriate level of cracking resistance [5, 6]. In this way, production routes involve (layer-by-layer) layup of prepregs, in which types and orientations of the reinforcing fibers significantly affect the static strength and the fatigue life of the laminates. These characteristics are improved when the fiber orientations coincide with the loading directions [7, 8], while the oblique layups (at an angle of 45°) enhance both the crack propagation resistance as well as the number of cycles to failure [9].

Conventionally, laminates are fabricated at low pressures by sintering stacked prepregs through the initiation of diffusion and interpenetration of polymer chains between adjacent layers, providing high values of Interlaminar Shear Strength (ILSS) [10, 11]. Homogeneous low-defect structures are ensured by both the steady-state pattern of the developing processes and the proper selection of polymer binders with specified level of viscosity in melted state [12]. However, such procedures are quite time consuming and expensive, so ultrasonic welding (USW) or ultrasonic consolidation might be implemented in some cases. Unfortunately, it is not always possible to ensure both homogeneity and low defectivity of the structures due to non-stationarity of the fabrication processes, high heating rates of nonlinear nature, and unilateral heat input during the energy transmission induced by ultrasonic vibrations. In fact, the 'sonotrode – stack of mated prepregs – rigid base's' oscillatory system should be considered for developing such production routs [13]. Correct selection of ultrasonic consolidation parameters ensures melting of polymers in the prepregs, primarily at the layer interfaces, while preserving the original structure and integrity of the reinforcing components (carbon fibers/CFs or CF fabrics). Since, the application of ultrasonic vibrations causes relative displacements of the joined layers, it is crucial to minimize melting of the thermoplastic binders within the prepregs.

As reported earlier [14, 15], USW of the laminates based on thermoplastic binders is conventionally realized by inserting energy directors (EDs) between them (for example, continuous films from neat polymers ~250 μm thick). Due to their negligible thickness, the EDs melt first and then partially extruded from the fusion zone. Typically, USW procedure is terminated when sonotrode is displaced over distances commensurate with the initial ED thickness [16, 17]. In such cases, thicknesses of the US-welded laminates (several millimeters) and their elastic moduli (units of GPa) are multiply greater than those of the EDs. As a result, frictional heat is generated primarily at the fusion zone. It should be noted that the quality of USW lap joints is assessed by measuring their ILSS values [18].

Nowadays, research activities are quite extensive in the highlighted direction, while the variable parameters include: i) types of the laminates (different proportions of various binders and reinforcing fibers); ii) shapes and materials of EDs; iii) USW process parameters, etc. [19].

The above reviewed references on US-welding address the problem of utilizing ultrasonic vibrations for assembling the components (fabrication of permanent joints). However, the potential of applying ultrasonic energy opens up prospects of ultrasonic additive manufacturing. This makes it possible to speed up the fabrication process since frictional heating might be achieved during fractions of a second. From the other hand, the non-stationary nature of the process demands for using prepreg technology for ultrasonic assisted fabrication of layered composites. In regard of laminates fabrication, one of the main goals is to consolidate (layer-by-layer) prepregs (e.g., the PEEK/CF ones) with thicknesses of about two hundred microns, ensuring their minimal melting and damaging. To achieve it, relationships between the ultrasonic consolidation parameters and both formed structures and mechanical properties of the joints should be determined taking into account previously reported patterns for joining the neat PEEK plates and the PEEK/CF prepregs [20, 21].

Based on the above, the aim of this study was to assess the effects of the ultrasonic consolidation parameters and the insertion of EDs from the commercially available PEEK film ~250 μm thick on the structure and mechanical properties of the layered composites (laminates) of the PEEK-based prepregs reinforced with unidirectional CFs.

As a null hypothesis, an assumption is made about the possibility of ultrasonic consolidation of prepregs without introducing energy director (ED) between the adjacent layers. For the sake of comparison, EDs in the form of an industrially manufactured PEEK film with a thickness of 250 microns were placed between sequentially ultrasonic consolidated prepregs.

MATERIALS AND METHODS

In this study, commercially available PEEK-based prepregs reinforced with tapes of unidirectional CFs (Fig. 1 a, c) (Toray Cetex TC1200; 160 μm thick, fiber areal weight – 145 g/m^2, resin content by weight – 34%, density – 1.59 g/cm^3) were ultrasonically consolidated (joined) with and without EDs from neat PEEK films (Fig. 1 b, d) (Victrex, Aptiv 2000; 250 μm thick, density – 1.26 g/cm^3) using an 'UZPS-7' USW machine (Fig. 2) (SpetsmashSonik LLC, Voronezh, Russia).

Rectangular shape pieces of the prepregs were placed in a clamp, minimizing the possibility of their relative movement. A sonotrode of a square cross-section of 20×20 mm provided ultrasonic vibrations to the prepreg layers being joined.

Ultrasonic vibrations with duration (t_{US}) from 600 up to 1200 ms were applied at a clamping force of 1.5 atm. After turning off ultrasonic vibrations, the clamping was kept lasting for 5000 ms (pressure holding time). The schematic of the ultrasonic consolidation process is shown in Fig. 3. The laminates without the EDs consisted of 16 prepreg layers (in doing so, 4 prepregs were consolidated at once), while 7 and 6 layers of the prepregs and the EDs respectively (3 prepregs and 2 ED

were consolidated (joined) at once) composed the samples of other kind; the different number of prepregs was motivated by the necessity to ensure similar thicknesses of the samples for the subsequent ILSS tests. At least four samples of each type were fabricated and tested. Because the total PEEK contents varied, the authors did not expect to achieve equal ILSS values since this study primarily aimed to form low-defect interfaces ensuring acceptable functional characteristics.

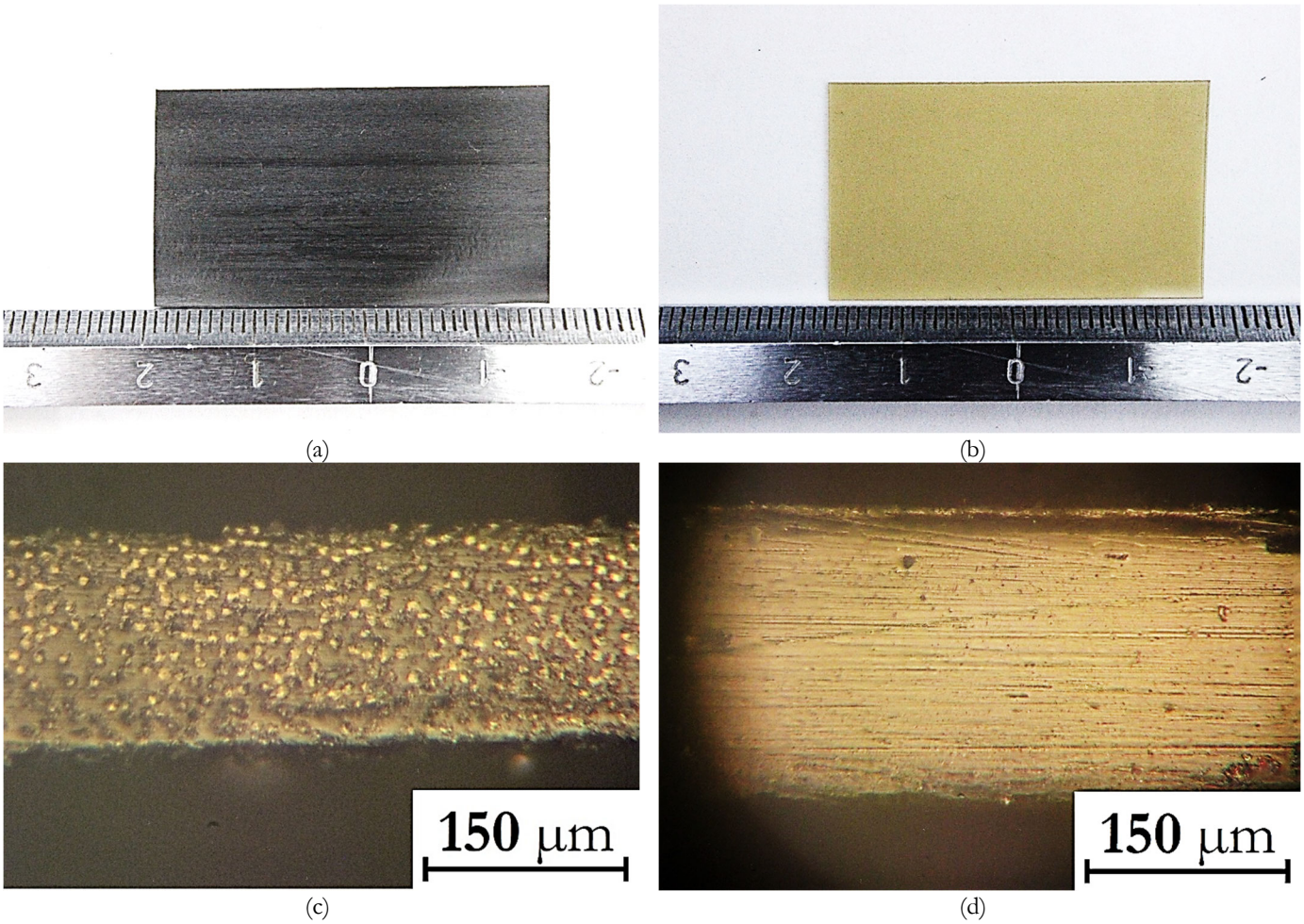

(a) (b) (c) (d)

Figure 1: Photographs of components used for samples' fabrication; a, b – top view; c, d – cross section; prepreg (a, c), neat PEEK-film (b, d).

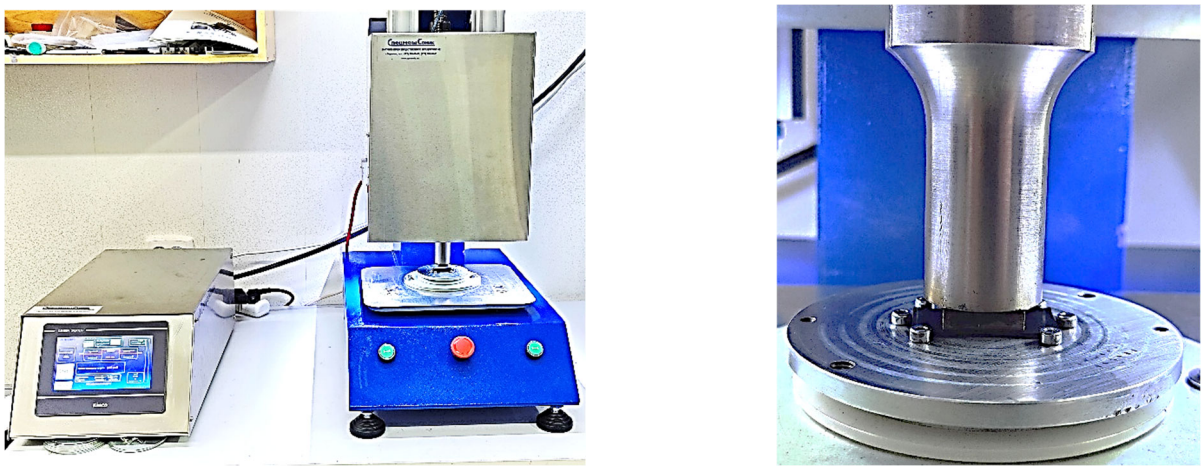

(a) (b)

Figure 2: Ultrasonic welding bench (a), welding setup on anvil (b).

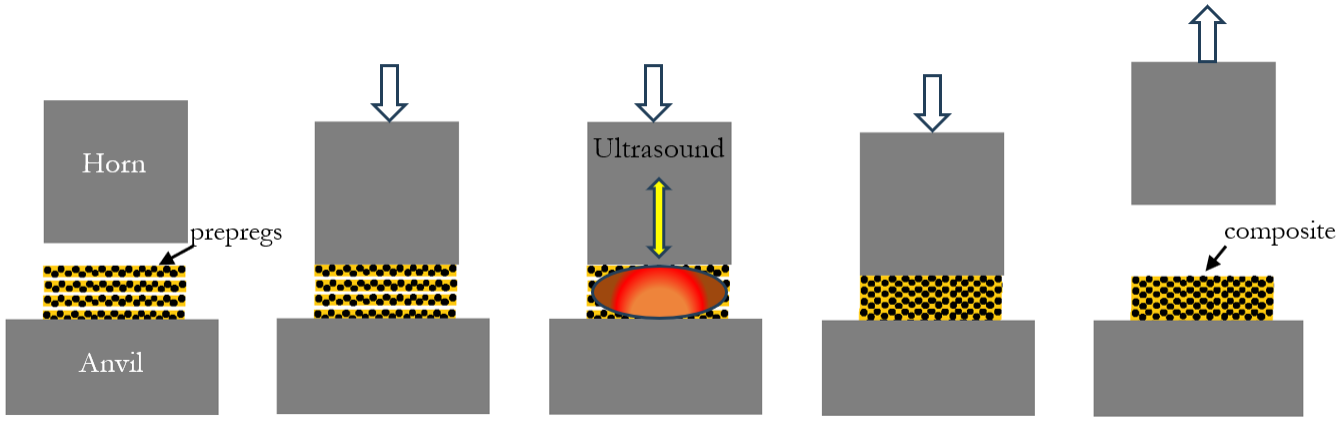

Figure 3: Schematic of ultrasonic consolidation of stacked prepregs.

The parallelepiped shaped samples for mechanical tests sized 12×4×2 mm³ were cut out from the ultrasonically consolidated laminate blanks with the help of CMC machine equipped with semicrystalline diamond cutting tool. The ILSS tests were carried out with an 'Instron 5582' (Instron, Norwood, MA, USA) electromechanical testing machine (Fig. 4). The span -to-thickness ratio was 8 mm, being equal to a product of specimen thickness (2.0 mm) by four. At least 4 samples of each type have been fabricated and tested. The cross head speed was 1 mm/min in order to meet the standard ASTM D2344.

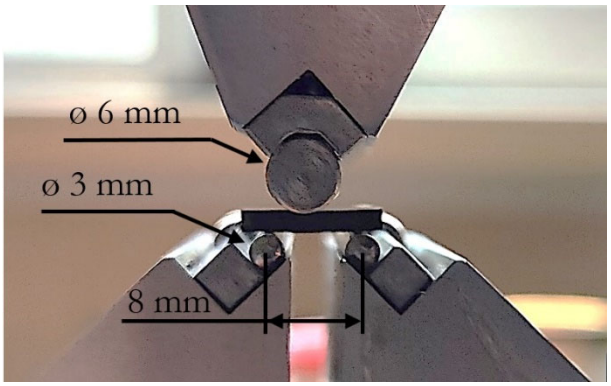

Figure 4: The photograph of the installation for the three-point bending test.

The apparent ILSS values were determined by the following equation:

$$ILSS = \frac{3}{4}\frac{F}{bh} \tag{1}$$

where $ILSS$ was interlaminar shear stress, MPa; F was load, N; b and h were width and thickness of a laminate, respectively, mm.

The cross section views of as fabricated and fractured samples were examined with the a "Neophot 2' optical microscope (Carl Zeiss Jena, Germany) equipped with a "Canon EOS 550D" digital camera (Canon Inc., Japan).

EXPERIMENTAL RESULTS

Fig. 5 shows the data on laminates' thinning versus duration of ultrasonic vibrations for both types of layered composites (with and without the EDs). For the ED-less laminates, the trend was characterized by a S-shape pattern with increasing time of application ultrasonic energy from 600 up to 800 ms. Under these conditions, the laminates' thinning values increased by 2.8 and 1.5 times, respectively compared to those of the layered composites with the EDs. When calculated over the number of the layers (prepregs only or prepregs+EDs), the thickness change per unit prepreg was

equal to 18 and 34 μm, respectively. Without the EDs, further prolonging the ultrasonic duration reduced the laminate's thinning below 300 μm.

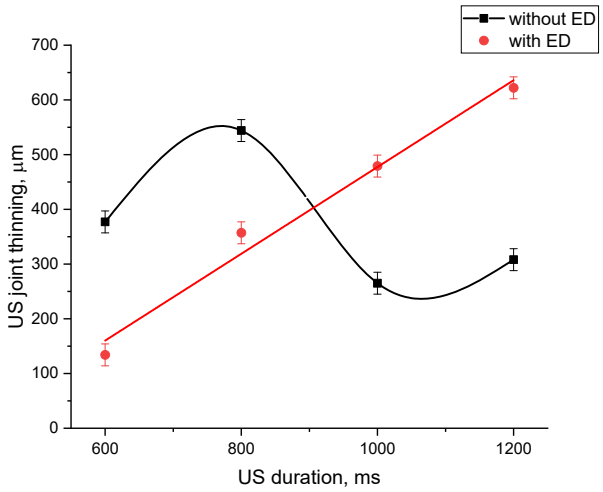

Figure 5: The thinning of laminates versus ultrasonic duration relationships for the layered composites with and without the Eds.

For the laminates with the EDs, the laminates' thinning increased with prolonging the ultrasonic application time. At its maximum value of t_{US}=1200 ms, the joints (laminates) thinned twice as much (by ~600 μm) compared to those without the EDs. Such a significant change was caused by both melting and extrusion of the EDs, as well as partial melting and deformation of the polymer binder in the prepregs.

Fig. 6 presents general top view of the laminates. Some extrusion of the components (EDs) was found around the sonotrode contact zones (for the layered composites with the EDs; marked by red arrows in Fig. 6, b and d). With prolonging the ultrasonic duration, no significant differences were observed in the sizes of the 'sonotrode traces' or in the polymer volumes extruded from the fusion zones, (Fig. 6, b and d), which may indicate a similarity in the development of the structure formation processes for the studied layered composites.

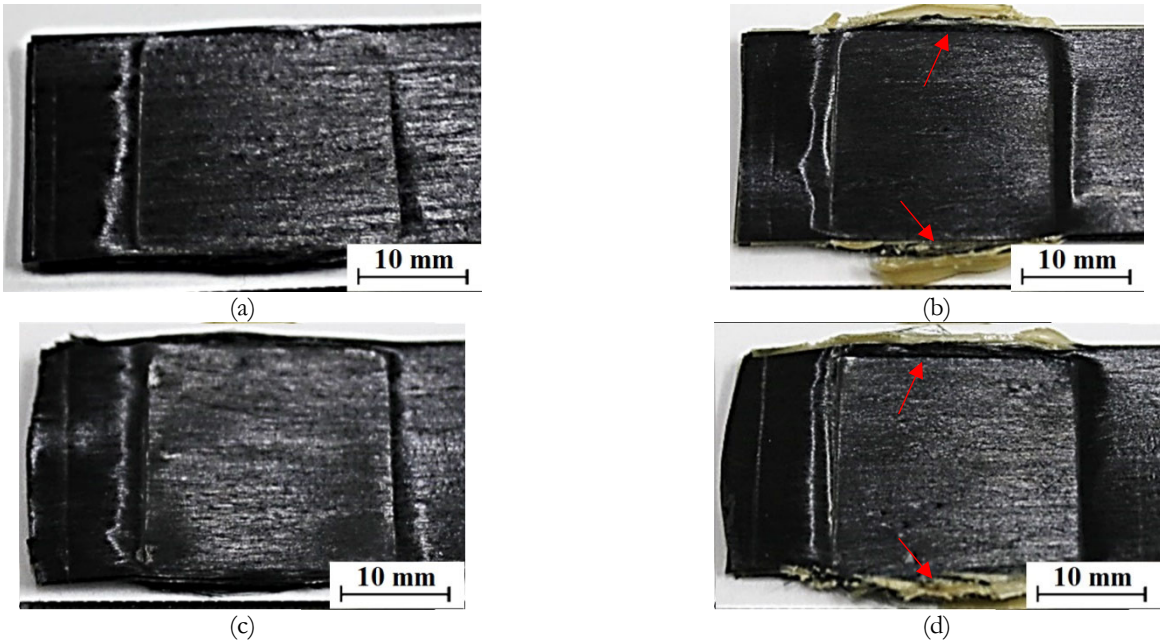

Figure 6: The general (top) views of the laminates: a) without the EDs, t_{US} = 600 ms; b) with the EDs, t_{US} =600 ms; c) without the EDs, t_{US} = 1200 ms; d) with the EDs, t_{US} = 1200ms.

Fig. 7 shows optical images of the cross-sections of the laminates. Without the EDs, their structure was fairly uniform and almost defect-free. The interfaces of individual prepregs were distinguishable only at the shortest ultrasonic duration of 600 ms (Fig. 7, a), while they could not be followed at its maximum value of 1200 ms (Fig. 7, c). With the EDs, both non-uniformity in the thicknesses of individual layers and their local curvature were observed at the shortest ultrasonic duration of 600 ms (Fig. 7, d), which was most likely caused by partial loss of structural integrity of each ED upon melting. At t_{US} = 800 ms, the EDs were thinner and more uniform, but there occurs localized failure of the original prepreg structures (Fig. 7, e). At the maximum ultrasonic duration of 1200 ms, some EDs were overpressed, while the prepregs were damaged (Fig. 7, e) due to intense melting, spreading, and extrusion of the EDs from the fusion zone.

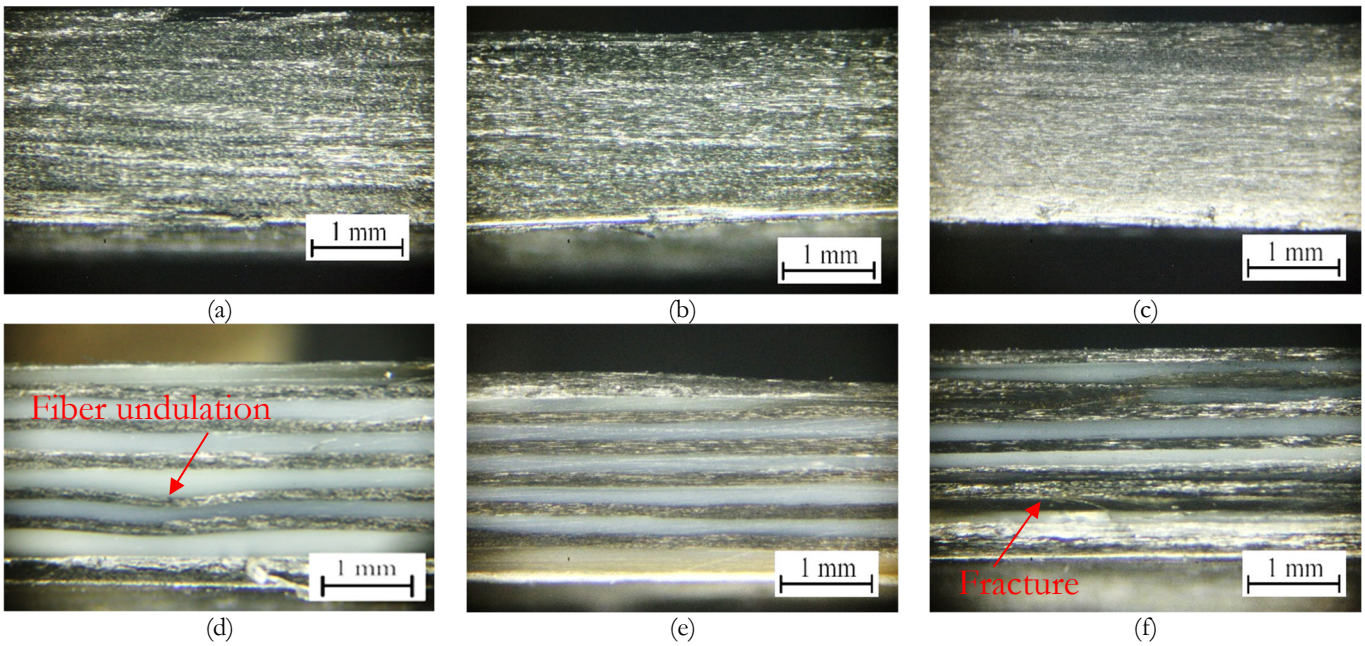

Figure 7: The optical images of the cross-sections of the joints: a) without the EDs, t_{US} = 600 ms; b) without the EDs, t_{US} = 800 ms; c) without the EDs, t_{US} = 1200 ms; d) with the EDs, t_{US} = 600 ms; e) with the EDs, t_{US} = 800 ms; f) with the EDs, t_{US} = 1200 ms.

Fig. 8 presents the ILSS versus ultrasonic duration relationships for the laminates under study. A greater scatter of the ILSS values was characteristic of those with the EDs, which was most likely caused by the pronounced heterogeneity of their structure. Without the EDs, prolonging the ultrasonic duration was accompanied by an increase in the ILSS values, the maximum of which corresponded to t_{US} = 1200 ms. With such prolongation of the ultrasonic duration, the ILSS values, conversely, decreased for the laminates with the EDs due to their more defective structures, including the presence of delaminations (Fig. 7, e).

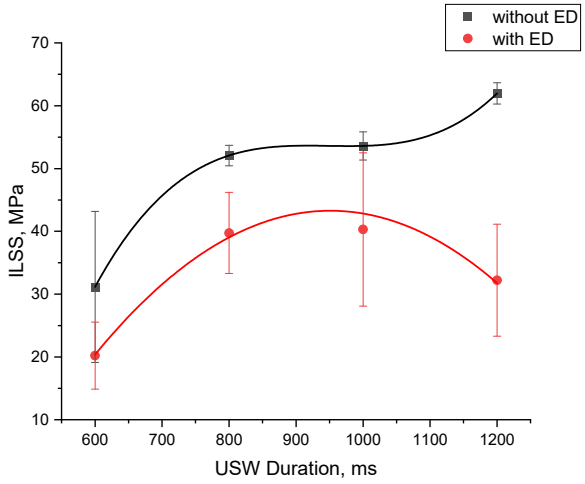

Figure 8: The ILSS versus ultrasonic duration relationships for the laminates with and without the EDs.

Fig. 9 shows optical images of the cross-sections of the fractured laminates after the ILSS tests. Without the EDs, the layered composites were fractured through the initiation and propagation of (adhesive) cracks at the prepregs' interfaces (Fig. 9, a–c). At the shortest ultrasonic duration of 600 ms, the number of such discontinuities was greater (Fig. 9, a), while the fracture patterns were visually less distinct with its prolongation (Fig. 9, b and c) and the layer interfaces remained virtually indistinguishable at t_{US} = 1200 ms (Fig. 9, c).

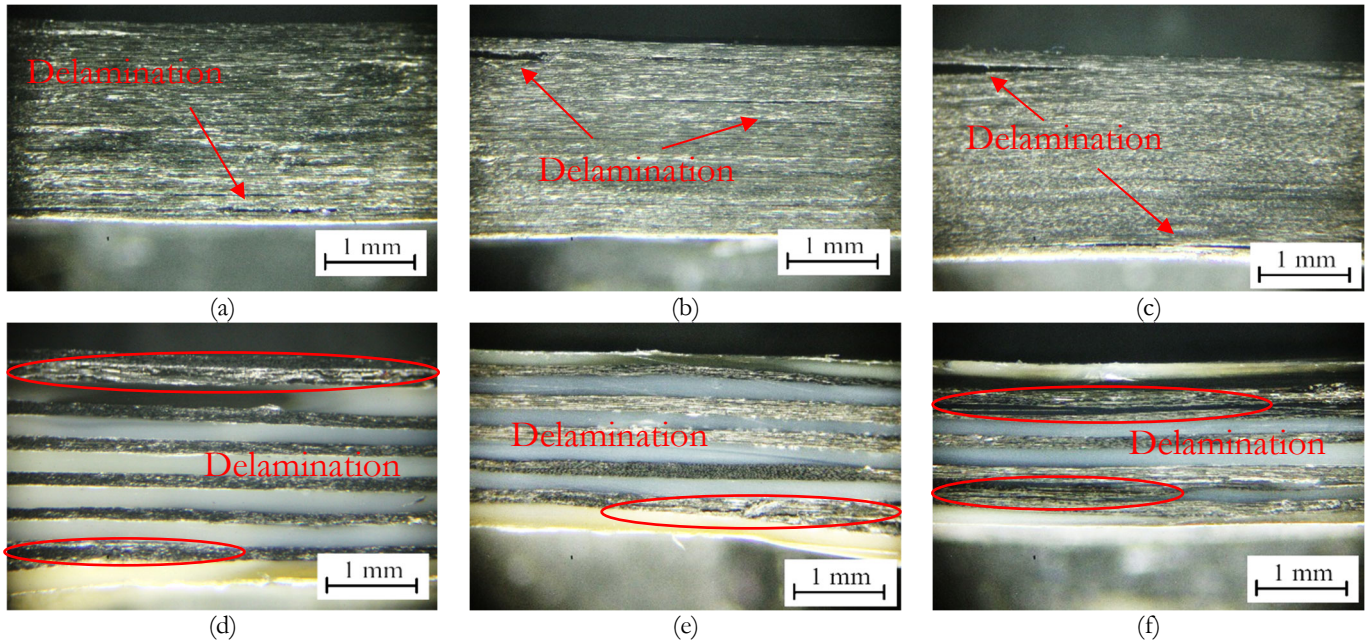

Figure 9: The optical images of the cross-sections of the fractured laminates after the ILSS tests: a) without the EDs, t_{US} = 600 ms; b) without the EDs, t_{US} = 800 ms; c) without the EDs, t_{US} = 1200 ms; d) with the EDs, t_{US} = 600 ms; e) with the EDs, t_{US} = 800 ms; f) with the EDs, t_{US} = 1200 ms.

With the EDs, the laminates were expectedly fractured along the interfaces between the prepregs and the EDs, but the failure types varied for different ultrasonic durations. At t_{US} = 600 ms, the layered composites fractured at a low ILSS value of ~20 MPa (Fig. 8) due to greater residual thicknesses of the ED layers and lower interlayer adhesion (Fig. 9, d). A more uniform and dense structure of the laminate formed at t_{US} = 800 ms possessed improved resistance to the initiation and propagation of cracks at the prepreg interfaces (Fig. 9, e) with an ILSS value of ~40 MPa (Fig. 8). At t_{US} = 1200 ms, local delaminations were observed already after the layered composite formation stage (as noted above), which contributed to the initiation and propagation of cracks along them via the interlayer shear mechanism (Fig. 9, f), so, the ILSS value decreased down to ~30 MPa (Fig. 8).

Fig. 10 presents optical images of the main crack propagation zones in the fractured laminates taken at a higher magnification. Without the EDs, the laminate fractured along the interfaces between the prepregs (at t_{US} = 600 ms, Fig. 10, a), confirming the insufficient level of adhesion between them (ILSS = ~32 MPa according to Fig. 8). At $t_{US} \geq$ 800 ms, cracks were characterized by branched propagation trajectories through adjacent joined prepregs (Fig. 10, b and c) at correspondingly high ILSS values of 50–60 MPa (Fig. 8).

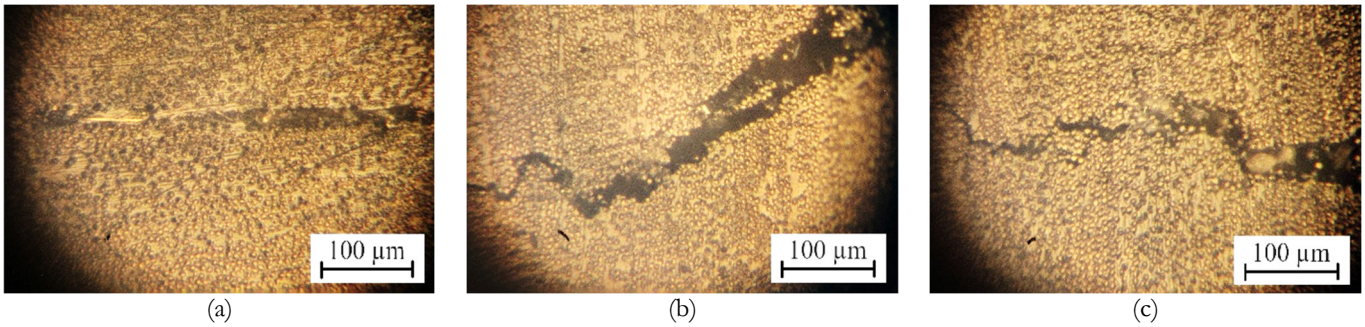

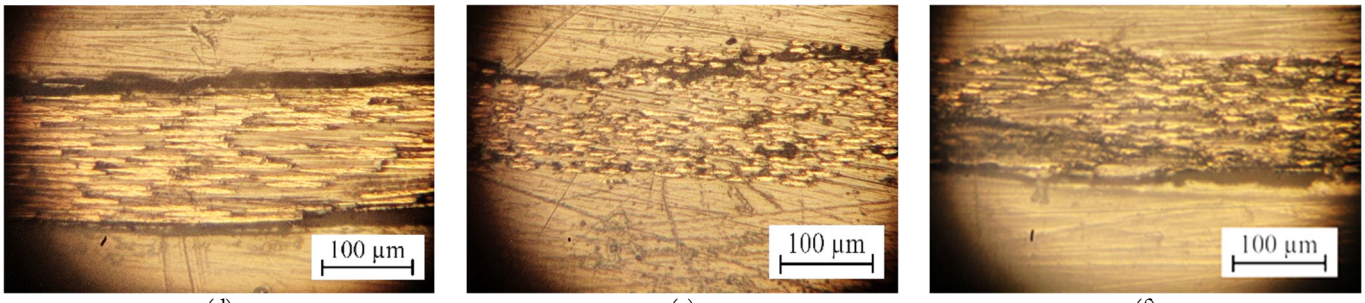

(d) (e) (f)

Figure 10: The optical images of the main crack propagation zones in the fractured laminates at the higher magnification: a) without the EDs, t_{US} = 600 ms; b) without the EDs, t_{US} = 800 ms; c) without the EDs, t_{US} = 1200 ms; d) with the EDs, t_{US} = 600 ms; e) with the EDs, t_{US} = 800 ms; f) with the EDs, t_{US} = 1200 ms.

With the EDs, all the laminates fractured through the interfaces between the EDs and the prepregs, which could be clearly seen in Fig. 10, d for t_{US} = 600 ms. At t_{US} = 800 ms, such interfaces did not contain any visually distinguishable discontinuities. This fact ensured the maximum ILSS value of ~38 MPa, and the trajectory of the main crack propagation along the layer interfaces (Fig. 10, d) was determined by the difference in their strength properties. At the maximum ultrasonic duration of 1200 ms, local delaminations were found even before the ILSS test due to partial penetration of the molten EDs into the prepregs on its both sides (Fig. 9, e). So, the main crack propagated both inside the prepreg and along its interface with the ED (Fig. 10, e), decreasing the ILSS value down to ~32 MPa.

DISCUSSION

The ultrasonic consolidation process involved four main stages. Firstly, the sonotrode was pressed against the surfaces of the joined prepreges until the required driving force has been reached. Secondly, the application of ultrasonic vibrations heated them. Thirdly, they were melted and deformed. Finally, ultrasonic vibrations were turned off and the joined layers cooled down under the applied pressure.

For occurring the molecular interdiffusion, temperatures of both amorphous and semicrystalline thermoplastic resins had to be higher than their melting points [22]. According to Zhang et al. [23], surface friction was the primary heating mechanism for thermoplastic resins from room temperature to the glass transition levels during the ultrasonic consolidation process. Then, surface friction gave rise to viscoelastic heating (a significantly faster heating mechanism). When using the EDs, the melting process was slower because they acted as dampers, absorbing some of the energy supplied from ultrasonic vibrations.

Fig. 11 shows dependences of both ED and prepreg thicknesses (for the laminates with the EDs) on the ultrasonic duration, obtained by analyzing the optical images. These data indicated that the EDs were barely deformed, maintaining their thicknesses close to the initial value at t_{US} = 600 ms. As the ultrasonic duration was prolonged, the ED thicknesses decreased linearly. However, the scatter of the thickness values was wide, indicating the heterogeneity of the formed layered structures (laminates).

At the same time, the prepreg thicknesses, conversely, increased linearly with prolonging the ultrasonic duration. It is suggested that this effect could be explained by damage to the prepregs due to 'pumping' of the molten EDs. At the ultrasonic durations of 1000 and 1200 ms, both prepreg melting and additional impregnation with the molten EDs occurred due to overheating caused by the transmitted energy of ultrasonic vibrations. As a result, the prepreg thicknesses exceeded the initial value of ~160 μm.

Without the EDs, partial melting of the prepregs was also possible at $t_{US} \geq 1000$ ms, not only at the contact surfaces (interfaces) but also within them. This fact could be evidenced by both the laminates' thinning (Fig. 4) and the interface blurring in the optical images (Figs. 7, b and 9, c). Thus, the maximum ILSS value of ~60 MPa at t_{US} = 1200 ms (Fig. 8) was caused mostly by damage to the original prepreg structures, which was a negative factor (unacceptable in practical applications). The scatter of the ILSS values was large for the ED containing laminates, indicating the heterogeneity of the formed layered structures. It is suggested that this effect could be explained by damage to the prepregs due to 'pumping' of the partly molten EDs during the ultrasonic consolidation.

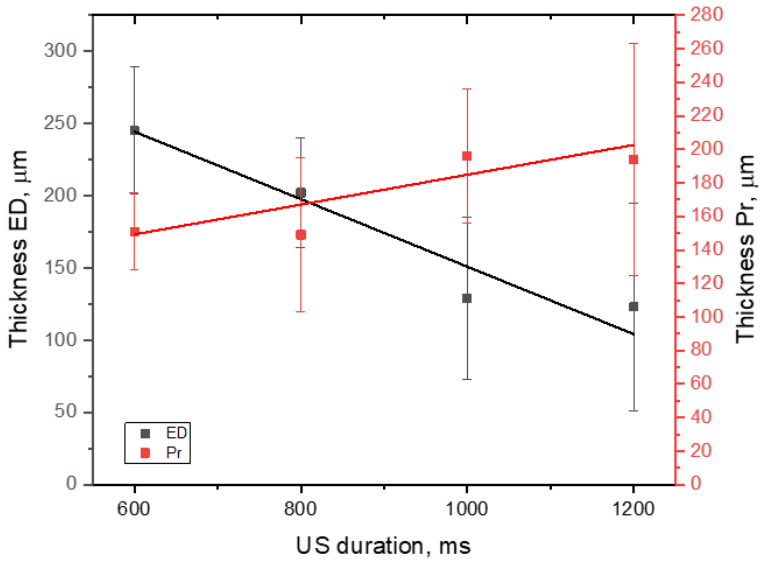

Figure 11: The dependences of both ED and prepreg (Pr) thicknesses (for the laminates with the EDs) on the ultrasonic duration.

For laminates manufacturing from industrially available prepregs, the approach without the use of the EDs should be considered to increase their ILSS values. The ultrasonic consolidation duration of 800 ms was the most rational, as it enabled to reduce the damaging effect of applied ultrasonic vibrations on the joined layers (prepregs), although the ILSS value did not reach the maximum level.

It should be noted that the ILSS values, obtained in this study for the joints (laminates) without the EDs, were lower by 40 % than those reported for the prepreg thermoforming method [24], and only by 10–25 % less for the laser automated fiber placement, implemented for similar unidirectional PEEK/CF prepregs [25, 26]. This fact reflected the potential of such production rout. In particular, the optimized variable parameter could be the amplitude of ultrasonic vibrations, the value of which was constant in this study (within 10 µm, while it was increased up to 80 µm by other researchers [27, 28]. In addition, a decrease in the sonotrode area could ensure a more uniform energy transfer to the fusion zones, which could be another subject of parametric optimizations.

Conclusions

The structures of the laminates of the unidirectional PEEK/CF prepregs with and without the EDs were formed differently during the ultrasonic consolidation processes. Such variations were determined either by melting and spreading of the binder alone within the prepregs (without the EDs) or by their simultaneous melting, spreading, and mixing. In the former case, prolonging the ultrasonic duration allowed for the prepreg interfaces to be virtually blurred, increasing the ILSS value up to the maximum level of 60 MPa (including due to localized damage to the prepregs).

With the EDs, excessive melting and spreading of the polymer occurred at the prolonged ultrasonic durations, increasing the number of discontinuities at the layer interfaces, including delaminations and the impregnation of the prepregs with the excessive binder. This fact was evidenced by the increase in their thicknesses relative to the initial value.

For laminates manufacturing from industrially available prepregs, the approach without the use of the EDs should be recommended. The ultrasonic duration of 800 ms was the most rational, as it enabled to reduce the damaging effect of applied ultrasonic vibrations on the joined layers (prepregs), increasing the ILSS value above 50 MPa. The latter exceeded the ILSS value of the laminates with EDs by 25 %.

Acknowledgments

The study was funded by the 24-79-00189 grant from the Russian Science Foundation. https://rscf.ru/project/24-79-00189. The authors acknowledge senior researcher of ISPMS SB RAS M.V. Burkov for providing PEEK/CF prepregs for fabrication of the samples.

REFERENCES

[1] Cao, Z., Zhan, L., Ma, B., Li, S., Xie, M. and Guo, J. (2025). The key technologies for fiber-reinforced polymer composites manufacturing: A state-of-the-art review, Thin-Walled Struct., 217, pp. 113773. DOI: https://doi.org/10.1016/j.tws.2025.113773.

[2] Dong, W., Karalis, G., Liebscher, M., Wang, T., Liu, P., Li, W. and Mechtcherine, V. (2025). Multifunctional carbon fibre reinforced polymer (CFRP) composites for sustainable and smart civil infrastructure: A comprehensive review, Sustainable Mater.Technol., 45, pp. e01594. DOI: https://doi.org/10.1016/j.susmat.2025.e01594.

[3] Bai, Q., Hao, Q., Dai, H., Chen, Y. and Dai, N. (2025). A review on integrated design and manufacturing technologies for continuous fiber-reinforced polymer composite lightweight structures in aerospace, Thin-Walled Struct., 217, pp. 113750. DOI: https://doi.org/10.1016/j.tws.2025.113750.

[4] Muliana, A., Nair, A., Khan, K. and Wagner, S. (2006). Characterization of thermo-mechanical and long-term behaviors of multi-layered composite materials, Compos. Sci. Technol., 66, pp. 2907–2924. DOI: https://doi.org/10.1016/j.compscitech.2006.02.016.

[5] Toroghinejad, M., Jamaati, R., Dutkiewicz, J. and Szpunar, J. A. (2013). Investigation of nanostructured aluminum/copper composite produced by accumulative roll bonding and folding process, Mater. Des., 51, pp. 274–279. DOI: https://doi.org/10.1016/j.matdes.2013.04.002.

[6] Chaudhari, G. and Acoff, V. (2009). Cold roll bonding of multi-layered bi-metal laminate composites, Compos. Sci. Technol., 69, pp. 1667–1675. DOI: https://doi.org/10.1016/j.compscitech.2009.03.018.

[7] Hazimeh, R., Challita, G., Khalil, K. and Othman, R. (2015). Experimental investigation of the influence of substrates' fibers orientations on the impact response of composite double-lap joints, Compos Struct., 134, pp. 82–89. DOI: https://doi.org/10.1016/j.compstruct.2015.08.040.

[8] Shi, H., Villegas, I.F. and Bersee, H.E.N. (2013). Strength and failure modes in resistance welded thermoplastic composite joints: Effect of fibre–matrix adhesion and fibre orientation, Compos. A Appl. Sci. Manuf., 55, pp. 1–10. DOI: https://doi.org/10.1016/j.compositesa.2013.08.008.

[9] Raimondo, A., Oca, I.U. and Bisagni, C. (2021). Influence of interface ply orientation on delamination growth in composite laminates, J. Compos. Sci., 55(27), pp. 3955–3972. DOI: https://doi.org/10.1177/00219983211031636.

[10] Gomer, A., Zou, W., Grigat, N., Sackmann, J. and Schomburg, W.K. (2018). Fabrication of Fiber Reinforced Plastics by Ultrasonic Welding, J. Compos. Sci., 2(3), pp. 56. DOI: https://doi.org/10.3390/jcs2030056.

[11] Lu, W., Yang, H., Dong, H., Chen, D. and Hu, J. Numerical and experimental study on the open-hole tensile properties of angle-ply carbon/glass hybrid laminates based on thin-ply carbon fiber prepreg, Compos. Struct., 372, pp. 119577. DOI: https://doi.org/10.1016/j.compstruct.2025.119577.

[12] Wang, H., Li, X., Phipps, M. and Li, B. (2022). Numerical and experimental study of hot pressing technique for resin-based friction composites, Compos. A Appl. Sci. Manuf., 153, pp. 106737. DOI: https://doi.org/10.1016/j.compositesa.2021.106737.

[13] Suna, Y., Liu, X. and Yang, X. (2018). A novel ultrasonic precise bonding with non-constant amplitude control for thermalplastic polymer MEMS, Ultrasonics, 84, pp. 404–410. DOI: https://doi.org/10.1016/j.ultras.2017.12.005.

[14] Sackmann, J., Burlage, K., Gerhardy, C., Memering, B., Liao, S. and Schomburg, W.K. (2015). Review on ultrasonic fabrication of polymer micro devices, Ultrasonics, 56, pp. 189–200. DOI: https://doi.org/10.1016/j.ultras.2014.08.007.

[15] Tsiangou, E., Kupski, J., Teixeira de Freitas, S., Benedictus, R. and Villegas, I.F. (2021). On the sensitivity of ultrasonic welding of epoxy- to polyetheretherketone (PEEK)-based composites to the heating time during the welding process, Compos. A Appl. Sci. Manuf.,144, pp. 106334. DOI: https://doi.org/10.1016/j.compositesa.2021.106334.

[16] Brito, C.B.G., Teuwen, J., Dransfeld, C.A. and Villegas, I.F. (2025). Ultrasonic welding of thermoplastic composites: A comparison between polyetheretherketone and low-melt polyaryletherketone as resin in the adherends and energy directors, Compos. B Eng., 296, pp. 112264. DOI: https://doi.org/10.1016/j.compositesb.2025.112264.

[17] Janek, M., Görick, D., Larsen, L., Jarka, S. and Kupke, M. (2025). Investigation of power and amplitude control in continuous ultrasonic welding of unidirectional CFRPs: A comparative study, Compos. A Appl. Sci. Manuf., 199, pp. 109194. DOI: https://doi.org/10.1016/j.compositesa.2025.109194.

[18] Liu, J., Quan, D., Wang, X., Yue, D., Pan, J. and Zhao, G. (2025). Enhancing the uniformity and strength of ultrasonically welded CF/epoxy-CF/PEI joints upon tailoring the structure of the energy director, Compos. B Eng., 294, pp. 112150. DOI: https://doi.org/10.1016/j.compositesb.2025.112150.

[19] Larsen, L., Endrass, M., Jarka, S., Bauer, S. and Janek, M. (2025). Exploring ultrasonic and resistance welding for thermoplastic composite structures: Process development and application potential, Compos. B Eng., 289, pp. 111927. DOI: https://doi.org/10.1016/j.compositesb.2024.111927.

[20] Alexenko, V., Panin, S.V., Stepanov, D.Yu., Byakov, A.V., Bogdanov, A.A, Buslovich, D.G., Panin, K.S. and Tian, D. (2023). Ultrasonic Welding of PEEK Plates with CF Fabric Reinforcement-The Optimization of the Process by Neural Network Simulation, Materials, 16(5), pp. 2115. DOI: https://doi.org/10.3390/ma16052115.

[21] Panin, S.V., Stepanov, D.Yu. and Byakov, A.V. (2022). Optimizing Ultrasonic Welding Parameters for Multilayer Lap Joints of PEEK and Carbon Fibers by Neural Network Simulation, Materials, 15(19), pp. 6939. DOI: https://doi.org/10.3390/ma15196939.

[22] Brito, C. B. G., Teuwen, J., Dransfeld, C.A. and Villegas, I. F. (2022). The effects of misaligned adherends on static ultrasonic welding of thermoplastic composites, Compos. A Appl. Sci. Manuf., 155, pp. 106810. DOI: https://doi.org/10.1016/j.compositesa.2022.106810.

[23] Zhang, Z., Wang, X., Luo, Y., Zhang, Z. and Wang, L. (2009). Study on Heating Process of Ultrasonic Welding for Thermoplastics, J. Thermoplast. Compos. Mater., 23(5), pp. 647–664. DOI: https://doi.org/10.1177/0892705709356493.

[24] Eremin, A.E, Burkov, M.V., Bogdanov, A.A., Kononova, A.A. and Lyubutin, P.S. (2024). Impact Behavior and Residual Strength of PEEK/CF-Laminated Composites with Various Stacking Sequences, Polymers, 16(5), pp. 717. DOI: https://doi.org/10.3390/polym16050717.

[25] Tobin, E., Ma, H., O'Higgins, R.M. and Weaver, P.M. (2025). Effect of automated tape placement pass frequency on matrix-dominated mechanical properties and microstructure of wound CF/PEEK, Compos. A Appl. Sci. Manuf., 194, pp. 108901. DOI: https://doi.org/10.1016/j.compositesa.2025.108901.

[26] Dong, N., Luan, C., Yao, X., Ding, Z., Ji, Y., Niu, C., Zheng, Y., Xu, Y. and Fu, J. (2024). Influence of process parameters on the interlaminar shear strength of CF/PEEK composites in-situ consolidated by laser-assisted automated fiber placement, Compos. Sci. Technol., 258, pp. 1109029. DOI: https://doi.org/10.1016/j.compscitech.2024.110902.

[27] Palardy, G., Shi, H., Levy, A., Corre, S.L. and Villegas, I.F. (2018). A study on amplitude transmission in ultrasonic welding of thermoplastic composites, Compos. A Appl. Sci. Manuf., 113, pp. 339–349. DOI: https://doi.org/10.1016/j.compositesa.2018.07.033.

[28] Tiwary, V.K., P, A. and Malik V.R. (2025). Ultrasonic Welding of Similar/Dissimilar MEX-3D Printed Parts Considering Energy Director Shape, Infill, Welding Time and Amplitude, Comput. Mater. Contin., 84(3), pp. 5111–5131. DOI: https://doi.org/10.32604/cmc.2025.066129.